

Physics of Spin Casting Dilute Solutions

Stefan Karpitschka,* Constans M. Weber, and Hans Riegler

Max-Planck-Institut für Kolloid- und Grenzflächenforschung, Potsdam-Golm, Germany

(Dated: February 9, 2019)

We analyze the spin casting of dilute (ideal) binary mixtures of non-volatile solutes in volatile solvents as a prototype for evaporation-controlled processes that are increasingly used to deposit specifically structured (sub)monolayers (“evaporation-induced self-assembly”). The first analytical description of the thinning of a volatile liquid film simultaneously subject to spinning and evaporation is presented. It shows, that the duration of a spin casting process is linked to the process parameters via power laws. A diffusion-advection model leads analytically to the equation governing the spatio-temporal evolution of the internal film composition. Its solution reveals that the solute concentration enrichment, its gradient, and its time evolution are related to the process parameters via power laws. The physics behind the power laws is uncovered and discussed. This reveals universal insights into the interplay between the control parameters and their impact on the spatio-temporal evolution of the film composition of diluted mixtures. It also offers palpable guidelines to better understand and control the spin casting of non-ideal solutions.

PACS numbers: 47.57.eb, 47.85.mb, 68.03.Fg, 82.70.-y

Introduction.—An excess amount of liquid deposited on a spinning, planar, wettable substrate flattens to a film of uniform thickness h . The film thins with time as the liquid flows outward and/or is spun off [1]. In addition, evaporative losses may contribute to film thinning. For an ideal (Newtonian) liquid this is described by [2]:

$$dh/dt = -2K h^3 - E, \quad (1)$$

with a spin-off coefficient $K = \omega^2/(3\nu)$, $\omega =$ rotational speed, $\nu =$ kinematic viscosity and $E =$ evaporation rate. Eq. 1 has not yet been solved analytically but numerical results and asymptotics reveal that, right after liquid deposition, hydrodynamic forces dominate and cause a rapid (nonlinear) film thinning (Fig. 1). Later, hydrodynamic thinning slows down and evaporative losses become dominant. Nonvolatile components remain as deposit on the substrate. Forming a persistent deposit this way is commonly denoted “spin casting/coating”.

Coverage, structure and properties of the final deposit are strongly influenced by the processes occurring *during* film thinning. The nonvolatile components get enriched until the concentrations exceed the saturation limits. The final deposit evolves from aggregation and/or precipitation during film thinning in the presence of the solvent. Most of the research regarding the spin cast process deals with polymer films, which also dominate its industrial application [3]. In this case *universal* insights into the spatio-temporal composition evolution within the film during spin casting remain unclear because polymeric solutions behave distinctively and non-ideally regarding rheology and evaporation.

Spin casting (film drying) is increasingly used to deposit specifically structured (sub)monolayers, e.g., specific particle arrays (“evaporation-induced self-assembly”) [4–12]. The spatio-temporal evolution of the non-volatile components (solute, (nano)particles) in

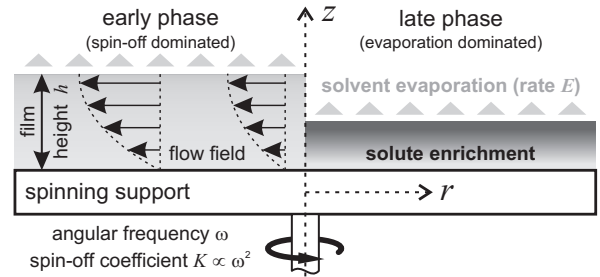


FIG. 1: Schematics of spin-casting with processes dominating early and late stages.

these cases can be prototyped as spin casting of dilute solutions.

We study analytically this prototype i.e., spin casting of ideal binary mixtures of a non-volatile solute and a volatile solvent. The analytical solution of Eq. 1 is presented for the first time. The spatio-temporal composition evolution of a binary mixture within such a film is then addressed with a diffusion-advection approach. We reveal power law relations between the experimental control parameters and the compositional evolution. This theoretical description is particularly valuable because the latter is experimentally hardly measurable but it determines solute nucleation, aggregation and growth i.e., the structure of the final deposit.

The results recommend spin casting of diluted solutions as a tool for fundamental studies on nucleation and growth under defined spatio-temporal constitutional conditions. They show how to understand and control coverage and structure of (sub)monolayer deposits [9, 13]. For dilute (approximately ideal) solutions our analysis is (semi-)quantitatively relevant. For real, non-ideal solutions it provides palpable guidelines toward controlled modifications.

Film thinning with evaporation.—The radial velocity field $u(r, z)$ of a Newtonian fluid rotating with its solid support (no slip), with a free surface at the top (no stress) is (irrespective of evaporation, [1]):

$$u(r, z) = 3K r z (h - z/2). \quad (2)$$

r and z are the radial respectively vertical coordinates in both lab- and rotating frame. The radial volumetric flux ϕdz is:

$$\phi dz = 2\pi r u(r, z) dz = 6\pi K r^2 z (h - z/2) dz, \quad (3)$$

With the continuity equation this yields the thinning-induced vertical motion of the horizontal stream lines:

$$\frac{dZ}{dt} = -\frac{1}{2\pi r} \int_0^z \partial_r \phi dz' = -K z^2 (3h - z). \quad (4)$$

The spin-off rate is equivalent to the time-dependent position of the topmost stream line $dZ/dt|_{z=h}$ [1]:

$$dh_s/dt = -2K h^3. \quad (5)$$

With a constant evaporation rate E in addition to hydrodynamic thinning, Eq. 5 becomes Eq. 1. This equation is nonlinear and inhomogeneous and has not been solved analytically. However its equivalent inverse ($h(t)$ is bijective) is essentially linear and of zeroth order:

$$dt/dh = -(2K h^3 + E)^{-1}. \quad (6)$$

Integrating Eq. 6 yields the solution to Eq. 1:

$$t(h) = \left\{ \pi\sqrt{3} + 2\sqrt{3} \arctan \frac{1 - 2h(2K/E)^{1/3}}{\sqrt{3}} + \log \left[1 - \frac{3h(2K/E)^{1/3}}{(1 + h(2K/E)^{1/3})^2} \right] \right\} / (6(2E^2K)^{1/3}), \quad (7)$$

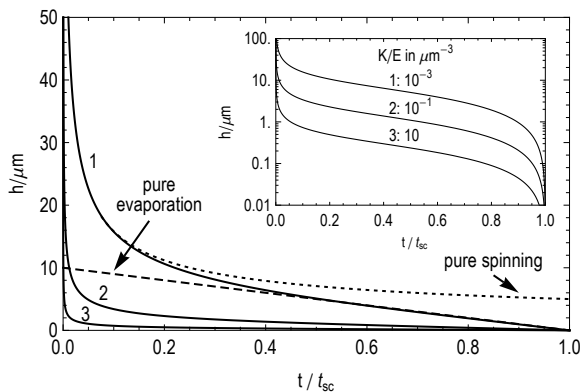


FIG. 2: Thinning curves $h(t)$ with t scaled by t_{sc} . Dotted line: $h(t)$ without evaporation. Dashed line: $h(t)$ without spinning off. $K/E = 10^{-3}(10^{-1}, 10) \mu\text{m}^{-3}$ corresponds to spin casting toluene at xxx rpm...

where the integration constant has been chosen such that $t = 0$ for $h \rightarrow \infty$. The duration t_{sc} of an “idealized” (starting at $h \rightarrow \infty$) spin casting process follows a power law of E and K :

$$t_{sc} = t(h \rightarrow 0) = 2\pi / \left(3\sqrt{3} (2E^2K)^{1/3} \right), \quad (8)$$

Fig. 2 shows $h(t)$ (Eq. 7) for different ratios K/E (the only parameter left after scaling t by t_{sc} [15]), compared to pure spinning off ($E = 0$, dotted) and pure evaporation ($K = 0$, dashed).

Solute concentration evolution.—Figure 2 shows that for typical experimental parameters a substantial part

of film thinning results from evaporation. Evaporation (drying) continuously enriches the nonvolatile solute. If we assume, as an approximation, that the *entire* casting is a drying process lasting for t_{sc} , this means drying a film of initial thickness $E \cdot t_{sc}$. With an initial solute concentration c_0 , this results in a final solute coverage $N(h \rightarrow 0)$ per area A [14]:

$$N(h \rightarrow 0)/A = c_0 E t_{sc} \propto c_0 (E/K)^{1/3}. \quad (9)$$

Solute enriches at the free surface (where the solvent evaporates). The enrichment spreads into the film via diffusion. Spinning-off (due to the shear flow) preferentially removes liquid from the surface region. Thus evaporative enrichment barely occurs in the beginning of the spin casting process and Eq. 9 provides an upper limit for the final solute coverage (for a better estimate see Eq. 18).

The spatio-temporal evolution of the solute concentration is described by:

$$\begin{aligned} \partial_t c &= D \partial_z^2 c - dZ/dt \partial_z c \\ &= D \partial_z^2 c + K z^2 (3h - z) \partial_z c, \end{aligned} \quad (10)$$

with an advective term due to the moving stream lines (Eq. 4). The boundary conditions for the solute concentration (Stefan condition at the free surface with evaporation, no diffusion through the substrate) are:

$$D \partial_z c|_{z=h} = E c|_{z=h}, \quad (11)$$

$$\partial_z c|_{z=0} = 0. \quad (12)$$

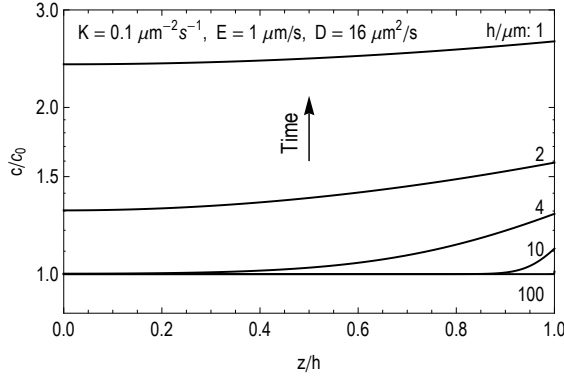


FIG. 3: Solute concentration profiles obtained by solving Eq. 15 (initial film thickness with homogeneous solute distribution $h = 110 \mu\text{m}$).

Rescaling with $y = z/h$ ($y \in [0, 1]$, from substrate to surface) avoids the moving boundary:

$$\begin{aligned} (\partial_t y) \partial_y c + \partial_t c = & D ((\partial_z^2 y) \partial_y c + (\partial_z y)^2 \partial_y^2 c) \\ & - \frac{dz}{dt} (\partial_z y) \partial_y c. \end{aligned} \quad (13)$$

Substituting explicit relations yields:

$$\partial_t c = \frac{D}{h^2} \partial_y^2 c + \left\{ \underbrace{\frac{K h^2 y^2 (3-y)}{h^2}}_{\text{advection due to stream line motion}} - \underbrace{\frac{y}{h} (2K h^3 + E)}_{\text{virtual advection due to scaling}} \right\} \partial_y c. \quad (14)$$

Eq. 14 describes the spatio-temporal evolution of the concentration as a function of t . $h(t)$ is required but not known explicitly, only its inverse, $t(h)$ (Eq. 7). Since $h(t)$ is bijective, the time variable can be changed to h : $\partial_t c = dh/dt \partial_h c = -(2K h^3 + E) \partial_h c$ (the dependence of c on h must not be confused with a specific coordinate; it is only an expression for time). With $\alpha = 2K/E$ and $\beta = D/E$ we obtain:

$$\partial_h c = -\frac{\beta h^{-2}}{\alpha h^3 + 1} \partial_y^2 c - \left\{ \frac{(hy)^2(3-y)}{2h^3 + 2/\alpha} - \frac{y}{h} \right\} \partial_y c, \quad (15)$$

with the appropriate free surface boundary condition:

$$\beta \partial_y c|_{y=1} = h c|_{y=1}. \quad (16)$$

Rescaling c by the initial solute concentration c_0 eliminates one more parameter and the initial condition is $c|_{h=h_0} = 1$. Essentially, the system is determined by 2 independent parameters (α and β). However, to keep physics palpable, we will stay with K , E , and D in the following. Eq. 15 can be solved numerically with h as independent variable [16]. Eq. 7 then provides the time to the corresponding h [17].

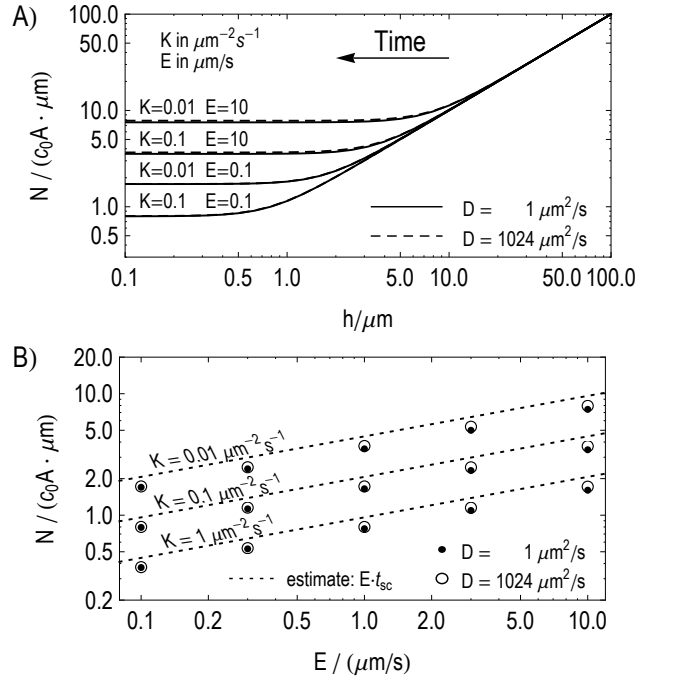


FIG. 4: Total solute amount per unit area (Eq. 17 applied to solutions of Eq. 15): A) as a function of film thickness (double logarithmic); B) final coverage as a function of evaporation rate E compared to the estimate Eq. 9.

General aspects of the concentration evolution.—In the following, based on solving Eq. 15, the effect of various parameters is analyzed in detail. For the analysis $h_0 = 110 \mu\text{m}$ was selected. Other $h_0 \in [50 \mu\text{m}, 500 \mu\text{m}]$ have also been tested. No significant impact on the results could be detected as long as $h_0 \gg E t_{sc}$.

Figure 3 shows snapshots of the solute concentration profile during film thinning for typical experimental parameters. First, a gradient in c develops only close to the surface ($h = 10 \mu\text{m}$). With thinner films ($h = 4 \mu\text{m}$), this gradient nearly reaches the substrate. Eventually the solute concentration increases globally ($h = 2 \mu\text{m}$), and finally the gradient decreases. Qualitatively this behavior reflects the interplay between evaporation (surfacial enrichment) and diffusion (equilibration over the film).

The total solute amount N per area A within a film of thickness h is:

$$\frac{N(h)}{A} = \int_0^h c dz = h \int_0^1 c dy, \quad (17)$$

This is plotted (normalized to c_0) as function of h in Fig. 4 A) for different K , D , and E . At the beginning (large h) there is virtually no global solute enrichment: $N(h)/A$ decreases proportional to the film thickness because all surficial solute enrichment is spun-off. Later (smaller h), spinning-off is less effective compared to evaporative enrichment. Solute diffuses into deeper film regions and $N(h)/A$ becomes increasingly independent

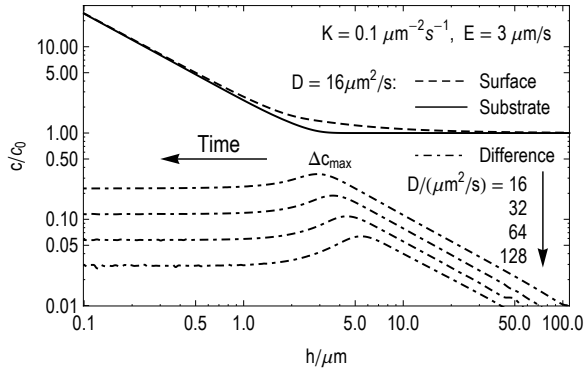


FIG. 5: Solute concentration at surface, substrate, and their difference. The maximum difference is correlated to the transition from spin-off to evaporation dominated thinning.

from $h(t)$. K and E essentially determine how $N(h)/A$ depends on h and how large the final solute coverage ($N(h \rightarrow 0)/A$) is, whereas D is less important (large D slightly augment $N(h)/A$).

The final coverage $N(h \rightarrow 0)/A$ is shown in Fig. 4 B) as function of E and K . The (numerical) data reveal a power law relation:

$$N(h \rightarrow 0)/A \approx 0.8 c_0 (K/E)^{-1/3}. \quad (18)$$

Except for the prefactor of ≈ 0.8 Eq. 18 is identical to Eq. 9 (which assumes only evaporation). The plot also reveals that the exponent slightly decreases for small D .

For the nucleation and growth of solute aggregates inside a thinning film, the spatio-temporal evolution of the solute concentration c is most important. Figure 5 shows c/c_0 at the free surface and at the substrate, respectively, as a function of h . As obvious from Fig. 3 these are the maximum respectively minimum values of c/c_0 for any given h . Also shown are the variations of the normalized difference $\Delta c/c_0 = (c(z=h) - c(z=0))/c_0$ as function of h for various D (the selected E and K are typical for toluene at 4200 rpm). For any given set of parameters K , E and D , a maximum, Δc_{max} , is found.

Figure 6 shows the spatio-temporal properties related to Δc_{max} as a function of D . The symbols represent the results from the numerical analysis. The lines depict the underlying power laws. These can be understood by analyzing the physics behind the solute enrichment as discussed in the following.

Panel A) shows the film thicknesses h_{max} corresponding to Δc_{max} . Δc_{max} emerges from a competition of evaporative enrichment against two antagonistic processes: spinning-off and diffusional equilibration. Both are relevant for opposite limits of h . For large h , surficial enrichment will be spun off, i.e. substantial Δc_{max} occurs only for $2K h_{max}^3 < E$ (from Eq. 1). On the other hand, for small h , diffusional equilibration is fast, requiring $D/h_{max} < E$ for significant Δc_{max} . Optimizing both relations simultaneously leads to the same power law as

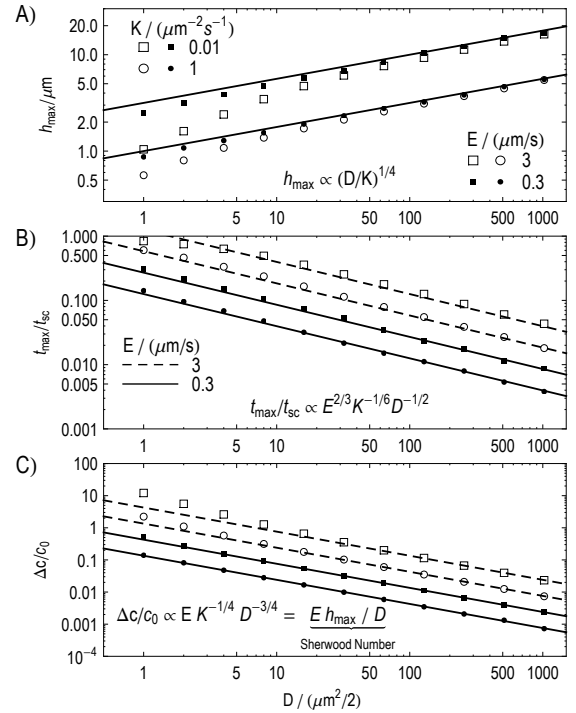


FIG. 6: Properties of the maximum concentration difference Δc_{max} as function of D : A) film height h_{max} , at which the maximum occurs, B) the corresponding reduced process time \tilde{t}_{max} , and C) the magnitude $\Delta c_{max}/c_0$.

the numerical analysis (which supplies the prefactor ≈ 1):

$$h_{max} \approx (D/K)^{1/4}. \quad (19)$$

E cancels out (it is linear and protagonistic in both cases).

Panel B) shows the rescaled time, t_{max}/t_{sc} , for h_{max} . Before reaching h_{max} , thinning is dominated by spinning-off. Hence t_{max} can be estimated by inserting h_{max} into $h = (2K t)^{-1/2}$ (the solution to Eq. 5). The result agrees with the numerical analysis (which provides the prefactor ≈ 0.28):

$$t_{max}/t_{sc} \approx 0.28 E^{2/3} K^{-1/6} D^{-1/2}. \quad (20)$$

$\Delta c_{max}/c_0$ (panel C) depends on the balance between evaporative (enriching) and diffusive (equilibrating) transport coefficients, i.e., the Sherwood number $Sh = E h_{max}/D$. With Eq. 19 this leads to (conform with the numerics, which contributes the prefactor ≈ 0.45)

$$\Delta c_{max}/c_0 \approx 0.45 E h_{max}/D = 0.45 E K^{-1/4} D^{-3/4}. \quad (21)$$

$\Delta c_{max}/c_0$ increases linearly with the evaporation rate E and decreases nearly as strong with the diffusion coefficient ($\propto D^{-3/4}$). The influence of the spinning rate is rather weak ($\propto K^{-1/4}$).

Conclusions.—We analyze the spin casting of ideal binary mixtures of a non-volatile solute and a volatile solvent to gain *universal* insights into the spatio-temporal

compositional evolution within the films. For the first time we present an analytical solution of the thinning of a volatile liquid film simultaneously subject to spinning and evaporation. Thus we find that the duration of a spin-casting process is linked to the process parameters by a power law. The compositional evolution of such a film is then studied via a diffusion-advection model. The resulting equations reveal general power law relations between the experimental control parameters (rotational speed, evaporation, and diffusion) and compositional parameters (final coverages, substrate/surface concentration difference). The physics background of the power laws is uncovered and discussed. It reveals universal insights into the interplay between the control parameters and their impact on the spatio-temporal evolution of the film composition. This is important because it determines solute nucleation, aggregation and growth i.e., the structure of the final deposit. Thus we present 1.) new quantitative insights into the (sub-)monolayer deposit formation from diluted (i.e., approximately ideal) mixtures, 2.) how spin casting can be used for nucleation and growth studies, and 3.) guidelines on how to influence the film evolution/coating properties in the case of spin casting non-ideal solutions (e.g. polymers).

We thank Andreas Vetter and John Berg for scientific discussions and Helmuth Möhwald for scientific advice and general support. SK was funded by DFG Grant RI529/16-1, CMW by IGRTG 1524.

* Electronic address: stefan.karpitschka@mpikg.mpg.de

- [1] A. G. Emslie, F. T. Bonner, and L. G. Peck, *J. Appl. Phys.* **29**, 858 (1958).
 [2] D. Meyerhofer, *J. Appl. Phys.* **49**, 3993 (1978).

- [3] K. Norrman, A. Ghanbari-Siahkali, and N. B. Larsen, *Annu. Rep. Prog. Chem. C* **101**, 174 (2005), in particular references 25 through 37 cited therein.
 [4] E. Rabani, D. R. Reichman, P. L. Geissler, and L. E. Brus, *Nature* **426**, 271 (2003).
 [5] T. P. Bigioni, X.-M. Lin, T. T. Nguyen, E. I. Corwin, T. A. Witten, and H. M. Jaeger, *Nat. Mater.* **5**, 265 (2006).
 [6] T. Hanrath, J. J. Choi, and D.-M. Smilgies, *ACS Nano* **3**, 2975 (2009).
 [7] A. T. Heitsch, R. N. Patel, B. W. Goodfellow, D.-M. Smilgies, and B. Korgel, *J. Phys. Chem. C* **114**, 1616 (2010).
 [8] E. Klecha, D. Ingert, and M. P. Pileni, *J. Phys. Chem. Lett.* **1**, 14427 (2010).
 [9] J. K. Berg, C. M. Weber, and H. Riegler, *Phys. Rev. Lett.* **105**, 076103 (2010).
 [10] A. C. Johnston-Peck, J. Wang, and J. B. Tracy, *Langmuir* **27**, 5040 (2011).
 [11] A. G. Marin, H. Gelderblom, D. Lohse, and J. H. Snoeijer, *Phys. Rev. Lett.* **107**, 085502 (2011).
 [12] M. A. Brookshier, C. C. Chusuei, and D. W. Goodman, *Langmuir* **15**, 2043 (1999).
 [13] H. Riegler and R. Köhler, *Nat. Phys.* **3**, 890 (2007).
 [14] D. E. Bornside, R. A. Brown, P. W. Ackmann, J. R. F. Frank, A. A. Tryba, and F. T. Geyling, *J. Appl. Phys.* **73**, 585 (1993).
 [15] $h(t)$ agrees well with experimental results, see supporting material.
 [16] Care has to be taken for errors from discretization, especially for boundary conditions. The initial condition has been slightly modified to be consistent with the boundary condition at the top surface (see supporting material).
 [17] Equivalently, Eq. 14 could be solved with numerically inverted $h(t)$; our method however reduces the dimension of the parameter space and optimizes computation time; the resulting abscissa can be converted to time using the analytical expression Eq. 7.